Spectral unmixing applied to fast identification of γ-emitting radionuclides using NaI(Tl) detectors

Hugues Paradis, Christophe Bobin, J. Bobin, Jacques Bouchard, Valérie Lourenço, Cheick Thiam, R. André, L. Ferreux, A. de Vismes Ott, M. Thévenin

SPECTRAL UNMIXING APPLIED TO FAST IDENTIFICATION OF γ-EMITTING RADIONUCLIDES USING NaI(Tl) DETECTORS

H. Paradis[a], C. Bobin[a*], J. Bobin[b], J. Bouchard[a], V. Lourenço[a], C. Thiam[a], R. André[a], L. Ferreux[c], A. de Vismes Ott[d], M. Thévenin[e]

[a]CEA, LIST, Laboratoire national Henri Becquerel, (LNE-LNHB), 91191 Gif-sur-Yvette Cedex, France
[b]CEA, IRFU, Laboratoire de cosmologie et statistiques, 91191 Gif-sur-Yvette Cedex, France
[c]IRSN, Laboratoire de mesures nucléaires, 78116 Le Vésinet Cedex, France
[d]IRSN, Laboratoire de métrologie de la radioactivité dans l'environnement, 91400 Orsay, France
[e]CEA, IRAMIS, Service de physique de l'état condensé, 91191 Gif-sur-Yvette Cedex, France

*Corresponding author
e-mail address: christophe.bobin@cea.fr
Tel.: +33 1 69 08 29 64

Keywords

Spectroscopic measurements, NaI(Tl) detector, environmental analysis, automatic decision-making, spectral unmixing, inverse problem, multiplicative update algorithm.

Abstract

Spectral unmixing was investigated for fast spectroscopic identification in γ-emitter mixtures at low-statistics in the case of measurements performed to prevent illegal nuclear material trafficking or for in situ environmental analysis following a radiological or nuclear accident. For that purpose, a multiplicative update algorithm based on full-spectrum analysis was tested in the case of a 3"x3" NaI(Tl) detector. Automatic decision-making was addressed using Monte Carlo calculations of decision thresholds and detection limits. The first results obtained with a portable instrument equipped with a 3"x3" NaI(Tl) detector designed for the control of food samples by non-expert users following a radiological or nuclear accident, are also presented.

1. Introduction

Fast and robust spectroscopic identification of γ-emitting radionuclides from radiation portal monitors (RPM) (e.g. located at borders) is key to prevent illegal nuclear material trafficking. The need for such identification algorithms is also important for in situ γ-ray measurements in environmental analysis following a radiological or nuclear accident. In these nuclear applications, the development of reliable automatic identification systems is essential to minimize the number of expert interventions in decision-making due to the large flow of measurements (Paff et al., 2017). For this

purpose, LNE-LNHB has developed an automatic identification algorithm based on spectral unmixing for fast anomaly detection of γ-emitting radionuclides in the presence of natural background radiation.

The fast identification code was first designed to meet the constraints related to measurements at low statistics (counting duration of a few seconds maximum) using RPMs equipped with scintillation detectors (plastic, NaI(Tl)). It was also developed to comply with real-time computing constraints in order to be implemented in embedded systems such as FPGAs (Field Programmable Gate Arrays) and microcontrollers. In order to be adapted to nuclear counting, the spectral unmixing code is based on a multiplicative update algorithm for maximum likelihood estimation with Poisson statistics. The aim of this algorithm is to estimate the composition of experimental γ-spectra on the basis of a linear mixture model of individual spectra of the γ-emitters to be identified (including natural background). As a result, each γ-emitter contribution (counting or mixing weight) is obtained without relying on intervention by an expert (e.g. without using region-of-interest (ROI) techniques).

A description of the spectral unmixing algorithm and its theoretical background based on Poisson statistics is presented, along with its validation carried out according to the specifications described in international standards and guidelines (ISO 22188:2004, 2004; IAEA NSS1, 2010; ANSI N42.38-2015, 2015) related to the use of RPMs for the prevention of illegal nuclear material trafficking. A dictionary of individual spectra measured using a classical a 3"x3" NaI(Tl) detector, was created with γ-emitting radionuclides covering a large range of energies between 40 keV and 2 MeV. The problem of decision-making is addressed by means of Monte Carlo calculations of decision thresholds. Detection limits were calculated and compared to international standards (IEC 62484:2010, 2010). The impact of γ-emitter mixtures on decision thresholds is also addressed. Finally, initial results are presented as obtained with a portable instrument based on a 3"x3" NaI(Tl) detector under development at IRSN/LMN for the control of food samples by non-expert users following a radiological or nuclear accident with releases. As an example, the counting durations required to achieve maximum permitted levels of radioactive contamination of food (Council regulation (Euratom) 2016/52) for ^{134}Cs, ^{137}Cs and ^{131}I were also calculated.

2. Linear spectral unmixing based on a multiplicative algorithm for maximum likelihood estimation with Poisson statistics

2.1 Multiplicative update rule for spectral unmixing

In γ-spectrometry the observed spectrum $\boldsymbol{s} = [s_1, \cdots, s_m]$ is composed of m samples or channels representing the distribution of γ-counting according to the deposited energy of interacting photons in a detector. Counting in channel i can be modeled according to a Poisson distribution depending on parameter λ_i, so that:

$$\forall i = 1,\cdots,m; \qquad \mathcal{P}(s_i = z) = \frac{\lambda_i^z}{z!}\exp(-\lambda_i) \qquad (1).$$

For spectral unmixing definition, the Poisson parameters λ_i are linear combinations of individual spectral signatures ϕ_i^k in channel i respectively related to the γ-emitting radionuclides (with index k) to be identified in a mixture and depending on the respective mixing weight a_k to be estimated. This entails that:

$$\forall i = 1,\cdots,m; \quad \lambda_i = \sum_{j=1}^{n} \phi_i^j \, a_j \qquad (2),$$

where n is the number of spectral signatures ϕ^k in a dictionary. From the above definitions, the likelihood of mixing weights a_k in channel i is defined as follows:

$$\forall i = 1,\cdots,m; \quad \mathcal{P}(s_i|a_1,\cdots,a_n) = \frac{\left(\sum_{j=1}^{n} \phi_i^j \, a_j\right)^{s_i}}{s_i!} \exp(-\sum\nolimits_{j=1}^{n} \phi_i^j \, a_j) \qquad (3).$$

When the m channels of the observed spectrum $\boldsymbol{s}$ are considered, the statistical independence of stochastic measurement process yields the following joint probability:

$$\mathcal{P}(s_1,\cdots,s_m|a_1,\cdots,a_n) = \prod_{i=1}^{m} \frac{\left(\sum_{j=1}^{n} \phi_i^j \, a_j\right)^{s_i}}{s_i!} \exp(-\sum\nolimits_{j=1}^{n} \phi_i^j \, a_j) \qquad (4).$$

Thus the maximum likelihood estimator of a single mixing weight a_k can be computed by minimizing the negative-loglikelihood $\mathcal{L}(a_k)$ as follows:

$$\forall k = 1,\cdots,n; \quad \hat{a}_k = \mathrm{argmin}_{a_k} \sum_{i=1}^{m} \left(\sum_{j=1}^{n} \phi_i^j a_j - s_i \log\left(\sum_{j=1}^{n} \phi_i^j a_j \right) \right) \qquad (5).$$

Assuming that $\forall i = 1,\cdots,m; \sum_{k=1}^{n} \phi_i^k a_k \neq 0$, the right expression is differentiable and its derivative is defined as follows:

$$\forall k = 1,\cdots,n; \qquad \nabla\mathcal{L}(a_k) = \sum_{i=1}^{m} \left(\phi_i^k - \frac{s_i}{\sum_{j=1}^{n} \phi_i^j a_j} \phi_i^k \right) \qquad (6).$$

The first-order optimality condition is given by $\nabla\mathcal{L}(\hat{a}_k) = 0$, which is equivalent to:

$$\forall k = 1,\cdots,n; \qquad \frac{1}{\sum_{i=1}^{m} \phi_i^k} \sum_{i=1}^{m} \frac{s_i}{\sum_{j=1}^{n} \phi_i^j \hat{a}_j} \phi_i^k = 1 \qquad (7).$$

Based on this optimality condition, each mixing weight a_k can be computed using a multiplicative update algorithm with non-negativity constraint (Lee and Seung, 2001) designed so that at each updating iteration ℓ:

$$\forall k = 1,\cdots,n; \qquad a_k^{(\ell+1)} = a_k^{(\ell)} \frac{1}{\sum_{i=1}^{m} \phi_i^k} \sum_{i=1}^{m} \frac{s_i}{\sum_{j=1}^{n} \phi_i^j a_j^{(\ell)}} \phi_i^k \qquad (8).$$

In the case where the spectral signatures are normalized, the multiplicative updating can be recast as:

$$\forall k = 1,\cdots,n; \qquad a_k^{(\ell+1)} = a_k^{(\ell)} \sum_{i=1}^{m} \frac{s_i}{\sum_{j=1}^{n} \phi_i^j a_j^{(\ell)}} \phi_i^k \qquad (9).$$

Considering the vectors representing the mixing weights $\boldsymbol{a} = [a_1,\cdots,a_n]$ to be estimated and the observed spectrum $\boldsymbol{s} = [s_1,\cdots,s_m]$ and the matrix $\boldsymbol{\Phi} = \left[\phi_i^k\right]$ of the normalized spectral signatures associated with each γ-emitting radionuclide to be identified, the multiplicative update rule can be expressed as follows:

$$\boldsymbol{a}^{(\ell+1)} = \boldsymbol{a}^{(\ell)} \odot \left(\boldsymbol{\Phi}^T \boldsymbol{s} \oslash \left(\boldsymbol{\Phi} \boldsymbol{a}^{(\ell)}\right)\right) \qquad (10)$$

where $\odot$ and $\oslash$ represent element-wise product and division respectively.

When using the multiplicative update rule (10) based on normalized spectral signatures, the estimated counting for each radionuclide k for a measured spectrum $\boldsymbol{s}$ are given by the estimator $\hat{a}_k$.

2.2 Validation tests using spectral signatures obtained with a 3''x3'' NaI(Tl) detector

Spectral unmixing using the multiplicative update rule expressed in (10) has the advantage to act as an effective compromise between speed and ease of implementation (Lee and Seung, 2001). It implicitly includes non-negativity constraints avoiding the estimation of non-physical negative counting. As depicted in Table 1, the first step of the algorithm consists in the definition of the initial values of the respective counting as the inverse of the number n of spectral signatures in a dictionary ($a_k^{(0)} = n^{-1}$). The iterative implementation of the multiplicative updating using expression (10), can be stopped when a maximum number of iterations is obtained or when the variation of the updated counting becomes lower than a defined value.

The multiplicative update algorithm allows a full-spectrum analysis without the use of region-of-interest windows. It can be applied according to either an off-line processing or a real-time implementation in which the estimated counting can be renewed during the spectrum measurement. It is worth noting that the multiplicative update rule is based on maximum likelihood estimation using a joint probability depending on the spectral signatures representing the detector response for a given γ-

emitting radionuclide. As a result, the spectral signature of natural background can also be considered in the multiplicative updating given in expression (10). It is thus possible to take into account the contribution of natural background in the statistical variability of the whole observed spectrum. When considering low-statistics measurements with significant contribution of natural background, this approach is better-suited than the conventional technique which consists in the substraction of the background from the observed spectrum (Laedermann et al., 2005).

The first validation tests were applied to identify potentially significant biases on estimated counting computed using the multiplicative update rule (10). In the present work, a dictionary of ten 1024-channel spectra (spectral signatures) was created representing the response of a 3"x3" NaI(Tl) detector measured for various γ-emitting radionuclides having photon emissions covering a large range of energies between 40 keV and 2 MeV (^{57}Co, ^{60}Co, ^{88}Y, ^{133}Ba, ^{134}Cs, ^{137}Cs, ^{152}Eu, ^{207}Bi, ^{237}Np, ^{241}Am). The choice of some γ-emitters was also relevant with radionuclides to be identified (^{57}Co, ^{60}Co, ^{137}Cs, ^{241}Am) as illicit radioactive material in international standards and guidance (ISO 22188:2004, 2004; IAEA NSS 1, 2010; ANSI N42.38-2015, 2015). According to IAEA NSS1 Technical Guidance (2010), where nuclear materials are specified for sensitivity testing, surrogate sources can be substituted. For instance, the surrogate for weapons grade plutonium is ^{133}Ba and for highly enriched uranium, it is ^{57}Co. Each individual γ-spectrum was measured using point sources placed at a distance of about 1 m from the 3"x3" NaI(Tl) detector without shielding (IEC 62484: 2010, 2010).

In a same manner as described for a previous study (Bobin et al., 2016), Monte Carlo calculations were implemented using theoretical spectra based on the experimental spectral signatures of each γ-emitter to be identified and their respective fractional contributions. The validation tests were performed by generating random spectra according to Poisson distributions with increasing mean total counting corresponding to typical low-statistics measurements (1000, 5000 and 10000 mean counts). The results presented in Table 2 were obtained in the case of a mixture of 5 γ-emitting radionuclides (^{57}Co, ^{60}Co, ^{88}Y, ^{137}Cs, ^{152}Eu) having strong overlaps between full-absorption peaks and Compton continuum. For each radionuclide, the fixed fractional contributions in the theoretical spectrum were respectively: ^{57}Co, 0.2; ^{60}Co, 0.2; ^{88}Y, 0.15; ^{137}Cs, 0.15; ^{152}Eu, 0.3. In Table 3, Monte Carlo calculations were implemented using a dictionary including the spectral signature of natural background in place of ^{237}Np. In that case, for each radionuclide to be identified and natural background, the fixed fractional contributions were respectively: background, 0.4; ^{60}Co, 0.15; ^{134}Cs, 0.05; ^{137}Cs, 0.15; ^{152}Eu, 0.25. The spectral unmixing code was also tested in the case of a higher mean value equal to 10^5 counts. For each mean total counting in Tables 2 and 3, the variability of the estimated counting was assessed by repeating the calculations 1000 times with different random spectra. The number of updating iterations to obtain the convergence of the multiplicative update algorithm was set equal to 10^3. For ease of comparison with expected fractional contributions in both

Tables 2 and 3, the estimated counting and their related standard deviations were divided by the mean values of total counting. The comparison between expected and estimated fractional contributions in Tables 2 and 3 obtained in the case of the mixture of 5 different spectral signatures, does not show significant biases even at low-statistics. It is noteworthy that the variances obtained by Monte Carlo calculations are higher than the estimated counting. Because of spectral unmixing, the standard deviations of the estimated counting associated with the radionuclides to be identified do not follow a Poisson distribution.

3. Decision-making: calculations of decision threshold and detection limit

False identification alarms when no γ-emitting source is present, are generally caused by statistical fluctuations in the counting of natural background. In the present study, the false positive rate in radionuclide identification was investigated by means of Monte Carlo calculations according to the definition of decision threshold in ISO 11929:2010 (2010). In Table 4, the decision thresholds (DT) are given for radionuclides used for RPM's testing (^{57}Co, ^{60}Co, ^{133}Ba, ^{137}Cs, ^{241}Am) as specified in the IEC 62484: 2010 standard (2010). They were obtained for an alpha risk of 10^{-3} (probability of error of first type (De Felice et al., 2017)) corresponding to a rate of 1 false identification for 1000 measurements of natural background. For that purpose, simulated background spectra were computed using a mean count equal to 1250 corresponding to measurements of 5 s. This duration is in the range of occupancy times when using RPMs for the detection of illegal radioactive materials. Calculations were implemented using the same dictionary comprising 10 spectral signatures as for the results given in Table 3. The DT values were determined from the distribution of the estimated counting obtained with the multiplicative update algorithm (10) when only natural background is considered. For each radionuclide, 10^5 background spectra were randomly calculated according to Poisson processes. Due to statistical fluctuations, non-zero counting can be obtained for a γ-emitter spectral signature. The DT values were estimated by considering that false identifications are equally and independently distributed among each radionuclide in the dictionary. As a result, after sorting the estimated counting in decreasing order, the DT value is given by the 11^{th} result in the calculated distributions for each γ-emitter spectral signature to meet the constraint of an alpha risk of 10^{-3}.

In the same manner, the detection limits (DL) related to false negative rates were determined according to a beta risk of 10^{-3} (probability of error of second type (De Felice et al., 2017)) for the same radionuclides (^{57}Co, ^{60}Co, ^{133}Ba, ^{137}Cs, ^{241}Am). In that case, Monte Carlo calculations were implemented using random spectra according to various mixtures of two spectral signatures (natural background and the radionuclide corresponding to the DL to be determined). After sorting the estimated counting in increasing order for the considered radionuclide, the DL value is determined from the optimized simulated mixture that yields the 100^{th} result (estimated counting) equal to the DT value previously obtained for the same radionuclide. In Table 4, the DL values were also calculated in

Bq unit considering detection efficiencies related to the full-spectrum measurements (unshielded sources placed at a distance of 1 m) and γ-intensities. These results are compared to the DL values calculated using the conventional ROI technique based on the main γ-photon emissions for each radionuclide (ISO 11929: 2010, 2010). The results in Table 4 clearly show that DL values can be significantly reduced when using full-spectrum analysis with the multiplicative update algorithm. The DL values are reduced by almost a factor equal to 3 in the case of ^{133}Ba and by a factor equal to 2 in the case of ^{60}Co. It is noteworthy that DT and DL values are significantly different between the considered radionuclides (^{57}Co, ^{60}Co, ^{133}Ba, ^{137}Cs, ^{241}Am). This behavior could be the result of correlations between radionuclides due to overlaps between spectral signatures covering different ranges of energies. A comparison between the estimated and simulated spectra is shown in Fig. 3 in the case of a mixture of natural background, ^{60}Co and ^{137}Cs with respective mean counting equal to 1250, 115 and 85. The two last expected counting correspond to the DL values of ^{60}Co/115 and ^{137}Cs/85 (see Table 4). DL values were also calculated in the case of a measurement duration equal to 1 s for ^{133}Ba and ^{60}Co. In both case, the DL values (180 kBq / ^{133}Ba and 130 kBq / ^{60}Co) remains significantly lower than the activities for RPM's testing (333 kBq / ^{133}Ba and 220 kBq / ^{60}Co) specified in IEC 62484: 2010 standard (2010).

The variation of DT values was also investigated by means of Monte Carlo calculations of mixtures with increasing counting of ^{60}Co with natural background. As depicted in Fig. 1, it can be remarked that the behaviour varies between the radionuclides considered (^{57}Co, ^{133}Ba, ^{137}Cs, ^{241}Am). It is clear that DT values related to ^{241}Am and ^{57}Co are less impacted by the increase of the counting due to the presence of ^{60}Co. On the contrary, the DT value associated to ^{137}Cs is more sensitive because of the large overlap existing between the ^{137}Cs spectrum and the ^{60}Co Compton continuum in the NaI(Tl) detector. This hypothesis is supported by the Monte Carlo simulations carried out with mixtures of increasing counting of ^{133}Ba with natural background. As shown in Fig. 2, the DT values related to ^{137}Cs and ^{60}Co are slightly impacted by the increasing counting of ^{133}Ba compared to the results given by ^{241}Am and ^{57}Co. The next step of the study will be a systematic investigation of the variation of DT values depending on the identified radionuclides and the dictionary used. This future work is essential to keep the alpha risk unchanged for automatic decision-making in the case of complex mixtures.

4. Application to the TRI-LATAC system developed at IRSN/LMN

The activities of IRSN (French Institute for Radiation Protection and Nuclear Safety) cover various domains such as radiation protection, nuclear safety and nuclear security in France. For this institute, a major radiological or nuclear accident could entail a critical situation requiring γ-spectrometry analysis of a huge number of environmental samples (Wei et al., 2018). In order to address this issue, a low-cost portable system based on a 3"x3" NaI(Tl) detector is under development at IRSN/LMN dedicated to in situ measurements for the control of food samples. The aim is to

combine this detection instrument (named TRI-LATAC) with automatic radionuclide identification for decision-making to enable non-expert users to implement a first screening of collected environmental samples. The system is composed of a cylindrical shielding made of steel (10-mm thickness) and lead (3-mm thickness) which surrounds the NaI(Tl) detector and the environmental sample to be analyzed. The spectral unmixing algorithm was tested in the case of the identification of ^{134}Cs, ^{137}Cs and ^{131}I according to the Council regulation 2016/52 (Euratom) defining maximum permitted levels (MPL) of radioactive contamination of food following a nuclear accident or any other case of radiological emergency. In the present work, the MPL values corresponding to infant food (150 Bq/kg for ^{131}I and 400 Bq/kg for both ^{134}Cs and ^{137}Cs) were considered for the Monte Carlo calculations of DT and DL.

A first dictionary of 7 spectral signatures (^{40}K, ^{131}I, ^{134}Cs, ^{137}Cs, ^{210}Pb, ^{241}Am, natural background) was created corresponding to the respective 3"x3" NaI(Tl) detector responses when measuring SG500 polyethylene containers (500 mL) filled with aqueous radioactive solutions. Except for ^{131}I, the spectral signatures were directly measured with the TRI-LATAC system using radioactive solutions with known activities prepared at LNHB. The counting rate related to natural background obtained at LNHB was equal to 75 s^{-1}. Regarding the spectral signature of ^{131}I, a geometrical modelling of the TRI-LATAC system (NaI(Tl) detector, SG500 container, shielding) was implemented with the Monte Carlo N-Particle eXtended (MCNPX) transport code (Breismeister, 2000). MCNPX simulations were validated using the measured spectral signatures obtained with the other γ-emitters (^{40}K, ^{134}Cs, ^{137}Cs, ^{210}Pb, ^{241}Am). Two additional dictionaries for the same radionuclides were also obtained by means of MCNPX simulations for two types of environmental samples (fresh plants and soils). Regarding simulations corresponding to fresh plants, calculations of spectral signatures were implemented using the chemical composition of cellulose (ρ=0.3 g.cm^{-3}; H, 48 %, O, 24 %, C, 28 %). In the case of soil samples, spectral signatures were calculated using the following chemical composition: ρ=1.3 g.cm^{-3}; H, 2 %, O, 57.5 %, Al, 8.5 %; Si, 26 %, Fe, 6 % (Bethesda, 1994).

For each radionuclide, DT and DL values were calculated according to alpha and beta risks equal to 2.5 % and for increasing measurement durations (30 s, 60 s, 120 s) in the same manner as previously described. The DL values for the γ-emitting radionuclides ^{134}Cs, ^{137}Cs and ^{131}I reported in Table 5 were determined using the full-spectrum detection efficiencies obtained experimentally or by means of Monte Carlo calculations. These results are displayed according to the types of environmental samples (aqueous solution, fresh plant, soil) and the measurement durations. It is clear from Table 5 that a counting duration of 30 s is sufficient to comply with MPL values specified for infant food in the Council regulation 2016/52 (Euratom) when applied to soil and aqueous samples. The measurement durations are longer in the case of samples made of fresh plants due to the lower density. Indeed, measurement durations of 2 min are needed to obtain a DL value below the MPL for

the sum of ^{134}Cs and ^{137}Cs contributions. A slightly longer duration is required in the case of ^{131}I. To summarize, a maximum duration of about 3 min is needed to comply with the MPL values specified in the most restrictive case of infant food for ^{134}Cs, ^{137}Cs and ^{131}I with regards to the 3 types of environmental samples. This result (lower than 5 min) complies with the expected duration values for a first screening based on in situ measurements following a major radiological or nuclear accident.

5. Discussion

First results of a spectral unmixing algorithm developed for fast decision-making using γ-spectrometry measurements at low-statistics with a 3"x3" NaI(Tl) detector, were presented. Based on a multiplicative update rule, the algorithm's originality lies in the fact that maximum likelihood estimation is based on a joint probability with Poisson statistics which accounts for the spectral signatures related to the γ-emitting radionuclides to be identified and also natural background. Combined to full-spectrum analysis, this property is important to take into account optimally the variability of the observed spectrum in decision-making at low-statistics. Contrary to classifiers such as artificial neural networks (Keller et al., 1995; Vigneron et al., 1996), the multiplicative update rule for spectral unmixing does not need a training phase based on a large dataset. The algorithm was first investigated in the case of the identification of radionuclides usually applied for RPM's testing (^{57}Co, ^{60}Co, ^{133}Ba, ^{137}Cs, ^{241}Am) for the prevention of illegal nuclear material trafficking. Detection limits determined by Monte Carlo calculations (alpha and beta risks equal to 0.1 %) for a 3"x3" NaI(Tl) detector are below the activities given in IEC 62484:2010 (2010) for counting durations in the range of a few seconds.

Regarding a real-time embedded implementation, the extraction of pulse amplitude and the spectrum accumulation could be performed according to a reconfigurable matrix in a FPGA and transmitted to an integrated microcontroller (a few hundreds of nanosecond is needed when using a 125-MHz 32-bit bus). Concerning the implementation of the multiplicative update algorithm in expression (10), one iteration requires n (dictionary dimension) multiplied by m (number of spectrum channels) multiply-and-accumulate (MAC) operations (1 clock cycle in simple precision, 2 clock cycles in double precision) (Cortex-A9 FPU, 2012). In the present paper, the maximum number of iterations for convergence was fixed to 1000. In the case of n and m respectively equal to 10 and 1024, approximately 10 million operations are needed. The lower bound of computing capacity of a single ARM processor in a low-cost Xilinx ZYNQ FPGA device is over 250 floating point MAC per second (double precision) and up to 2 GFlops when the "neon" vector extensions are used (Smith and Hamilton, 2015). As a result the maximum execution time for real-time implementation is approximately 40 ms (double precision) which is fully compatible with measurement durations in the range of a few seconds with RPMs.

Promising results were obtained with the TRI-LATAC system (equipped with a 3"x3" NaI(Tl) detector) developed at IRSN/LMN for the control of food samples by non-expert users after a radiological or nuclear accident with releases. Indeed a maximum measurement duration of about 3 min is sufficient to comply with the MPL values specified for infant food in the Council regulation 2016/52 (Euratom) for ^{134}Cs, ^{137}Cs and ^{131}I in the case of 3 different types of environmental samples (aqueous solution, soil, fresh plant). In the future, the study of the spectral unmixing algorithm will be extended to plastic detectors and liquid scintillation for environmental measurements. To this end, it will be essential to investigate the influence of correlations due to overlaps between spectral signatures.

References

ANSI N42.38-2015, 2015. American National Standards, Performance Criteria for Spectroscopy-based Portal Monitors Used for Homeland Security, IEEE.

Bobin, C., Bichler, O., Lourenço, V., Thiam, C., Thévenin, M., 2016. Real-time radionuclide identification in γ-emitter mixtures based on spiking neural network. App. Radiat. Isot. 109, 405-409.

Bethesda, M., 1994. Gamma ray spectrometry in the environment. ICRU Report n°53.

Breismeister, J.F., 2000. ″MCNP : a General Monte Carlo N-particle Transport code″

Cortex-A9 FPU, 2012. Cortex™-A9 Floating-Point Unit. Technical Reference Manual. https://static.docs.arm.com/ddi0408/i/DDI0408I_cortex_a9_fpu_r4p1_trm.pdf

De Felice, P., Jerome, S., Petrucci, A., 2017. Practical implementation of ISO 11929:2010. App. Radiat. Isot. 126, 256-262.

IAEA NSS 1, 2010. Technical Guidance, Technical and Functional Specifications for Border Monitoring Equipment, Reference Manual. IAEA, Vienna, Nuclear Security Series No. 1, revision 1.

IEC 62484: 2010, 2010. Radiation protection instrumentation - Spectroscopy-based portal monitors used for the detection and identification of illicit trafficking of radioactive material.

ISO 11929: 2010, 2010. Determination of the Characteristic Limits (Decision Threshold, Detection Limit and Limits of the Confidence Interval) for Measurements of Ionizing Radiation – Fundamentals and Application.

ISO 22188: 2004, 2004. Monitoring of inadvertent movement and illicit trafficking of radioactive material.

Keller, P., Kangas, L., Troyer, G., Hashem, S., Kouzes, R., 1995. Nuclear spectral analysis via artificial neural networks for waste handling. IEEE Trans. Nucl. Sci. 42 (4), 709–715.

Keshava, N., Mustard, J.F., 2002. Spectral Unmixing. IEEE Signal Processing Mag. 19, 44-57.

Laedermann, J.P., Valley, J.F., Bochud, F.O., 2005. Measurement of radioactive samples: application of the Bayesian statistical decision theory. Metrologia 42, 442-448.

Lee, D.D., Seung, H.S., 2001. Algorithms for Non-negative Matrix Factorization. Advances in Neural Information Processing Systems 13, 556-562.

Paff, M.G., Di Fulvio, A., Clarke, S.D., Pozzi, S.A., 2017. Radionuclide identification algorithm for organic scintillator-based radiation portal monitor. Nucl. Instrum. Methods A 849, 41–48.

Smith, J.W., Hamilton, A., 2015. Massive affordable computing using ARM processors in high energy physics. Journal of Physics: Conference Series 608 012001, 1-5.

Vigneron, V., Morel, J., Lépy, M.C., Martinez, J.M., 1996. Statistical modelling of neural networks in γ-spectrometry. Nucl. Instrum. Methods A 369, 642–647.

Wei, C., Garnick, K., Scott, T., Malkin, E., Szymanski, J., Laskos, S., Raimondi, J., Cocks, J., Morris, K., Mueller, W., Zickefoose, J., 2018. A portable real-time in situ gamma-ray analysis system. App. Radiat. Isot. 134, 157-162.

Table captions

Table 1: Multiplicative update algorithm in the case of a stopping criterion based on a maximum number of iterations

Table 2: Comparison between estimated and expected fractional contributions of γ-emitters in simulated mixtures with the following values: ^{57}Co, 0.2; ^{60}Co, 0.2; ^{88}Y, 0.15; ^{137}Cs, 0.15; ^{152}Eu, 0.3.

Table 3: Comparison between estimated and expected fractional contributions of γ-emitters (including natural background) in simulated mixtures with the following values: background (Bkg), 0.4; ^{60}Co, 0.15; ^{134}Cs, 0.05; ^{137}Cs, 0.15; ^{152}Eu, 0.25.

Table 4: Decision thresholds (DT) and detection limits (DL) for radionuclides used for RPM's testing. Monte Carlo calculations correspond to a measurement duration of 5 s using a mean counting rate equal to 250 s^{-1} for natural background in a 3"x3" NaI(Tl) detector without shielding. The detection limits were converted in Bq to be compared to the results based on the ROI technique (ISO 11929: 2010, 2010) and to activities of testing sources specified in IEC 62484: 2010 (2010).

Table 5: Evolution of detection limits (^{131}I, ^{134}Cs, ^{137}Cs) with the TRI-LATAC system for 3 counting durations according to 3 types of environmental samples (aqueous solution, fresh plants, soil). The results are compared with maximum permitted levels (MPL) of radioactive contamination of food (150 Bq/kg for ^{131}I and 400 Bq/kg for the sum of ^{134}Cs and ^{137}Cs contributions) given in the Council regulation 2016/52 (Euratom) for infant food.

Figure captions

Figure 1: Evolution of decision thresholds for ^{57}Co, ^{133}Ba, ^{137}Cs, ^{241}Am in the case of a mixture of natural background (250 s^{-1}) and increasing counting of ^{60}Co. The values correspond to a measurement of 5 s.

Figure 2: Evolution of decision thresholds for ^{57}Co, ^{60}Co, ^{137}Cs, ^{241}Am in the case of a mixture of natural background (250 s^{-1}) and increasing counting of ^{133}Ba. The values correspond to a measurement of 5 s.

Figure 3: Comparison between the estimated and simulated spectra in the case of a mixture of natural background, ^{60}Co and ^{137}Cs with respective mean counting equal to 1250, 115 and 85 for a measurement of 5 s with a 3"x3" NaI(Tl) detector without shielding. The two last values correspond to the detection limits of ^{60}Co/115 and ^{137}Cs/85 (counting rate 250 s^{-1} for natural background). The full-absorption peaks are respectively: 662 keV/^{137}Cs (channel 250), 1173 keV/^{60}Co (channel 433), 1332 keV/^{60}Co (channel 490) and 1461 keV/^{40}K (channel 543).

Table 1

Input
Spectral signatures of each γ-emitter to be identified: $\boldsymbol{\Phi} = \left[\phi_i^k\right]$ with $k = 1..n$
Experimental spectrum: $\boldsymbol{s} = [s_1,\cdots,s_m]$
Initialization
Maximum number of iterations: p_{max}
Definition of initial counting: $a_k^{(0)} = n^{-1}$
While $p < p_{max}$ **do**
Multiplicative updating of the estimated counting: $\boldsymbol{a}^{(p+1)} = \boldsymbol{a}^{(p)} \odot \left(\boldsymbol{\Phi}^T \boldsymbol{s} \oslash \left(\boldsymbol{\Phi}\boldsymbol{a}^{(p)}\right)\right)$
end
Output
Estimated counting for each γ-emitter to be identified

Table 2

Counts	^{88}Y/0.15	^{137}Cs/0.15	^{57}Co/0.2	^{241}Am/0	^{134}Cs/0	^{152}Eu/0.3	^{207}Bi/0	^{133}Ba/0	^{60}Co/0.2	^{237}Np/0
1000	0.149(23)	0.146(19)	0.200(20)	0.001(2)	0.007(11)	0.285(41)	0.003(6)	0.0045(79)	0.200(27)	0.004(7)
5000	0.150(10)	0.149(9)	0.200(10)	0.0005(8)	0.0034(49)	0.293(20)	0.0013(25)	0.0021(37)	0.199(12)	0.0019(33)
10000	0.150(7)	0.149(6)	0.200(7)	0.0004(6)	0.0023(35)	0.295(13)	0.0010(17)	0.0014(25)	0.200(9)	0.0013(22)
100000	0.150(2)	0.150(2)	0.200(2)	0.0001(2)	0.0007(10)	0.299(4)	0.0003(6)	0.0005(8)	0.200(3)	0.0005(7)

Table 3

Counts	Bkg/0.4	^{241}Am/0	^{133}Ba/0	^{207}Bi/0	^{57}Co/0	^{60}Co/0.15	^{134}Cs/0.05	^{137}Cs/0.15	^{152}Eu/0.25	^{88}Y/0
1000	0.382(40)	0.002(3)	0.008(12)	0.0055(88)	0.009(12)	0.152(24)	0.052(21)	0.152(20)	0.233(39)	0.004(6)
5000	0.394(18)	0.0009(13)	0.0033(47)	0.0025(38)	0.0035(46)	0.151(11)	0.05(1)	0.150(9)	0.244(18)	0.0017(23)
10000	0.395(13)	0.0006(9)	0.0023(33)	0.0017(26)	0.0026(33)	0.151(7)	0.051(7)	0.150(6)	0.245(13)	0.0011(16)
100000	0.398(4)	0.0002(3)	0.0008(10)	0.0006(8)	0.0009(10)	0.150(2)	0.050(2)	0.150(2)	0.248(4)	0.0004(5)

Table 4

	DT (5s)	DL (5s)	DL (kBq)	$DL_{ISO11929}$(kBq)	$A_{Testing}$ (kBq)
^{241}Am	28	60	97	148	1740
^{133}Ba	82	160	63	177	333
^{57}Co	57	110	54	89	555
^{60}Co	48	115	36	71	260
^{137}Cs	37	85	59	97	590

Table 5

	DL / Bq.kg^{-1} (30 s)			DL / Bq.kg^{-1} (60 s)			DL / Bq.kg^{-1} (120 s)			MPL / Bq.kg^{-1}
	Soil	Fresh plant	Aqueous solution	Soil	Fresh plant	Aqueous solution	Soil	Fresh plant	Aqueous solution	
^{134}Cs	77	356	101	53	242	69	37	169	48	400
^{137}Cs	105	461	133	71	310	90	49	216	62	
^{131}I	84	369	107	68	300	87	41	179	52	150

Figure 1

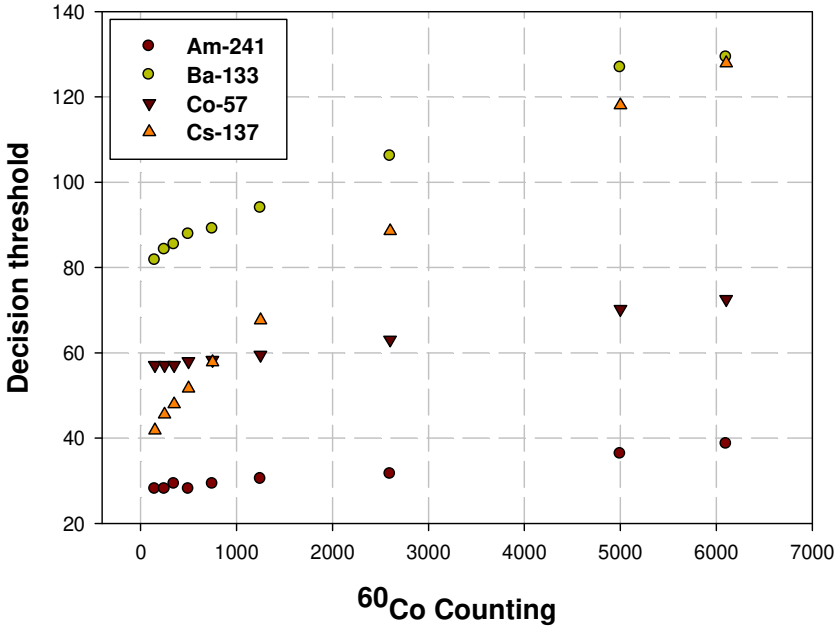
Am-241
Ba-133
Co-57
Cs-137
Decision threshold
60Co Counting
140
120
100
80
60
40
20
0
1000
2000
3000
4000
5000
6000
7000

Figure 2

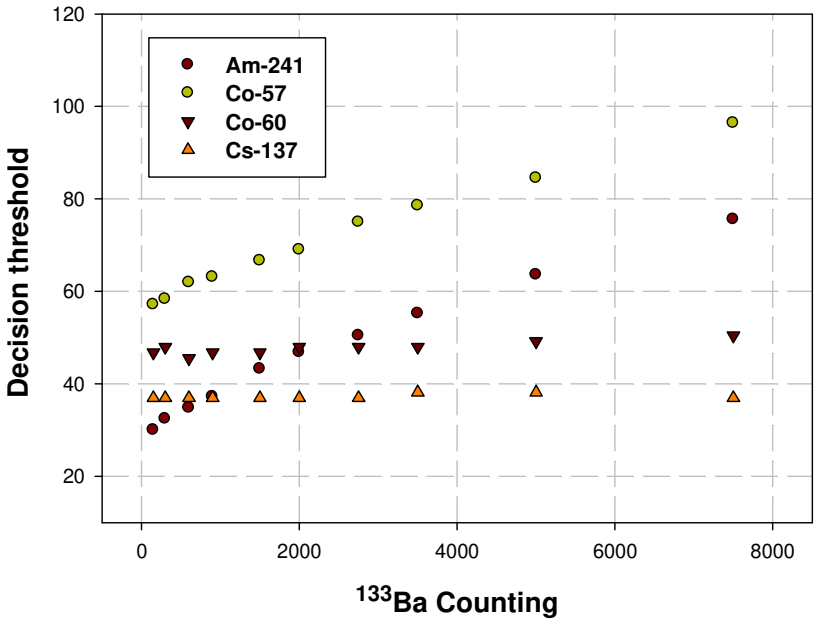
Am-241
Co-57
Co-60
Cs-137
Decision threshold
120
100
80
60
40
20
0
2000
4000
6000
8000
133Ba Counting

Figure 3

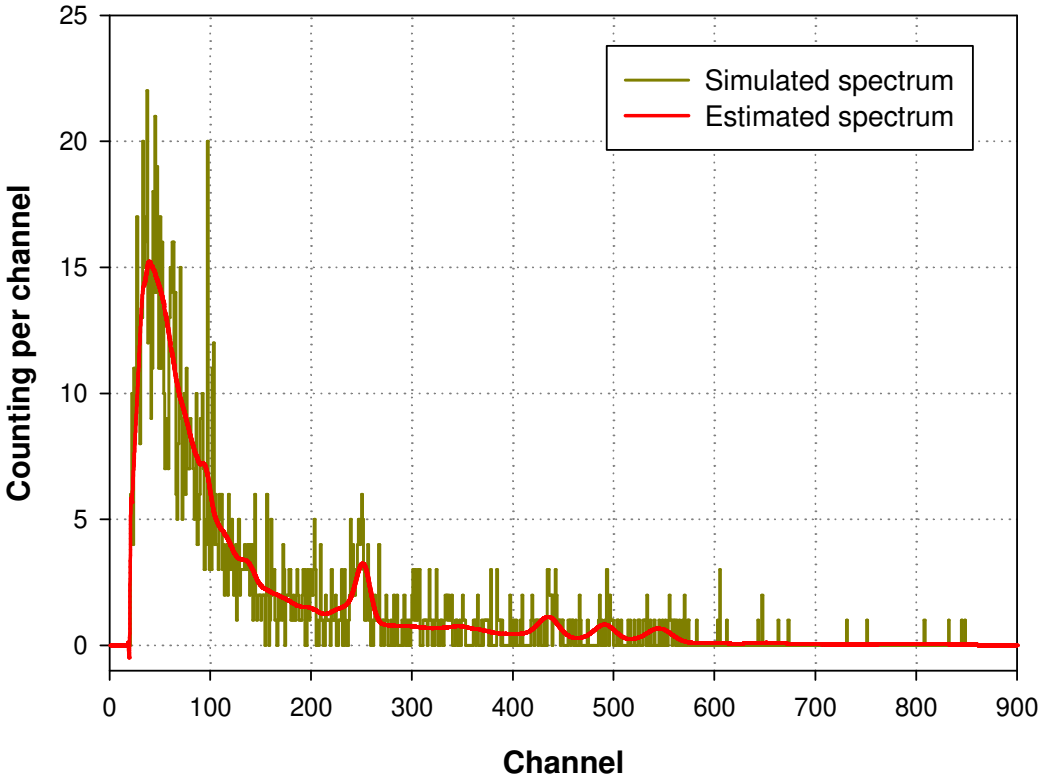
Simulated spectrum
Estimated spectrum
Counting per channel
Channel
0
5
10
15
20
25
0
100
200
300
400
500
600
700
800
900